

Quantifying the Genetics of Disease Inheritance With a Bayesian Perspective

Dylan Lawless^{*1}

¹Department of Intensive Care and Neonatology, University Children’s
Hospital Zürich, University of Zürich, Switzerland.

March 25, 2025

Abstract

We developed an integrative framework to quantify the probability of observing disease-associated variants across the genome by analysing large-scale annotation databases and curated gene panels. By combining reference population allele frequencies, ClinVar variant classifications, and inheritance patterns through rigorous Hardy-Weinberg-based calculations, our method estimated observation probabilities for each single nucleotide variant (SNV) and aggregated these probabilities by gene and variant classification. To demonstrate, we applied our approach to a disease gene panel associated with primary immunodeficiency and monogenic inflammatory bowel disease, resulting in 54,814 ClinVar variant classifications across 557 genes. Our results closely matched observed case counts in validation cohorts for both autosomal dominant (*NFKB1*) and autosomal recessive (*CFTR*) disorders, and provided robust priors for Bayesian models of variant and disease risk estimation. These findings demonstrated that integrating high-quality genomic annotations with classical genetic principles can enhance variant interpretation and support more precise clinical decision-making.

1 Introduction

In this study, we focused on reporting the probability of disease observation through genome-wide assessments of gene–disease combinations. Our central hypothesis was that by leveraging highly curated annotation data—including population allele frequencies, disease phenotypes, inheritance patterns, and variant classifications—and

^{*}Addresses for correspondence: Dylan.Lawless@kispi.uzh.ch

by applying rigorous calculations based on Hardy–Weinberg equilibrium (HWE), we could accurately estimate the expected probabilities of observing disease-associated variants.

Quantifying the risk that a newborn inherits a disease-causing variant is a fundamental challenge in genomics. Classical statistical approaches grounded in HWE (1; 2) have long been used to calculate genetic inheritance probabilities for single nucleotide variants (SNVs). However, applying these methods becomes more complex when accounting for different modes of inheritance, such as autosomal recessive (AR) versus autosomal dominant (AD) or X-linked (XL) disorders. In AR conditions, for example, the occurrence probability must incorporate both the homozygous state and compound heterozygosity, whereas for AD and XL disorders, a single pathogenic allele is sufficient to cause disease.

We argue that our integrated approach is highly powerful because the resulting probabilities can serve as informative priors in a Bayesian framework for variant and disease probability estimation—a perspective that is often overlooked in clinical and statistical genetics. Such a framework not only refines classical HWE-based risk estimates but also has the potential to enrich clinicians’ understanding of what to expect in a patient and to enhance the analytical models employed by bioinformaticians.

PanelAppRex is a novel tool developed to aggregate disease gene panel data from multiple sources—including GE PanelApp, ClinVar, and UniProt—and to facilitate sophisticated, natural language-based searches for clinical and research applications (16). It automatically retrieves and integrates gene panels, such as those used in the NHS National Genomic Test Directory and the 100,000 Genomes Project, into machine-readable formats that support rapid variant discovery and interpretation. By enabling queries based on gene names, phenotypes, and disease groups, PanelAppRex streamlines the process of identifying disease-associated variants and enhances the efficiency of genomic diagnostics. Critical details regarding its development and performance can be found in (17? ?).

dbNSFP is a comprehensive database designed for the functional prediction and annotation of all potential non-synonymous single-nucleotide variants (nsSNVs) and splicing-site SNVs in human protein-coding genes (18). It includes over 83 million variants and aggregates prediction scores from 34 different algorithms, conservation scores from 9 methods, and allele frequencies from major population datasets. Additionally, it provides extensive gene-related information from multiple resources, making it an invaluable tool for researchers assessing variant impact and disease association.

ClinVar is a public archive of human genetic variation that provided detailed classifications—such as “Pathogenic,” “Likely pathogenic,” and “Benign”—accompanied by supporting evidence and review status (17). It aggregated submissions from multiple sources to present both consensus and conflicting interpretations, mapped variants to reference sequences according to HGVS standards, and collaborated with expert panels like ClinGen for ongoing re-evaluation. Data from ClinVar was accessible via the website, FTP, and APIs for a range of clinical and research applications.

2 Methods

2.1 Variant Class Observation Probability

Our computational pipeline estimated the probability of observing a disease-associated genotype for each variant and aggregated these probabilities by gene and ClinVar classification. This approach included all variant classifications-not limited solely to those deemed “pathogenic”-and explicitly conditioned the classification on the given phenotype, recognising that a variant could only be considered pathogenic relative to a defined clinical context. The core calculations proceeded as follows:

1. Allele Frequency and Total Variant Frequency. For each variant i in a gene, the allele frequency was denoted as p_i . For each gene, we defined the total variant frequency (summing across all reported variants in that gene) as:

$$P_{\text{tot}} = \sum_{i \in \text{gene}} p_i.$$

If a variant had no observed allele ($p_i = 0$), we assigned a minimal risk:

$$p_i = \frac{1}{\max(AN) + 1},$$

where $\max(AN)$ was the maximum allele number observed for that gene. This adjustment ensured that a nonzero risk was incorporated even in the absence of observed variants.

2. Occurrence Probability Based on Inheritance. The probability that an individual was affected by a variant depended on the mode of inheritance relative to a specific phenotype. Specifically, we calculated the occurrence probability $p_{\text{disease},i}$ for each variant as follows:

- For **autosomal dominant (AD)** and **X-linked (XL)** variants, a single copy was sufficient, so

$$p_{\text{disease},i} = p_i.$$

- For **autosomal recessive (AR)** variants, disease manifested when two pathogenic alleles were present. In this case, we accounted for both the homozygous state and the possibility of compound heterozygosity:

$$p_{\text{disease},i} = p_i^2 + 2p_i(P_{\text{tot}} - p_i).$$

3. Expected Case Numbers and Case Detection Probability. Given a population with N births (e.g. as seen in our validation studies, $N = 69\,433\,632$), the expected number of cases attributable to variant i was calculated as:

$$E_i = N \cdot p_{\text{disease},i}.$$

The probability of detecting at least one affected individual for that variant was computed as:

$$P(\geq 1)_i = 1 - (1 - p_{\text{disease},i})^N.$$

4. Aggregation by Gene and ClinVar Classification. For each gene and for each ClinVar classification (e.g. “Pathogenic”, “Likely pathogenic”, “Uncertain significance”, etc.), we aggregated the results across all variants. The total expected cases for a given group was:

$$E_{\text{group}} = \sum_{i \in \text{group}} E_i,$$

and the overall probability of observing at least one case within the group was calculated as:

$$P_{\text{group}} = 1 - \prod_{i \in \text{group}} (1 - p_{\text{disease},i}).$$

5. Data Processing and Implementation. We implemented the calculations within a high-performance computing (HPC) pipeline and provided an example for a single dominant disease gene, *TNFAIP3*, in the source code to enhance reproducibility. Variant data were imported in chunks from the annotation database for all chromosomes (1–22, X, Y, M).

For each data chunk, the relevant fields were gene name, position, allele number, allele frequency, ClinVar classification, and HGVS annotations. Missing classifications (denoted by “.”) were replaced with zeros and allele frequencies were converted to numeric values. We then retained only the first transcript allele for simplicity, as the analysis was based on genomic coordinates. Subsequently, the variant data were merged with gene panel data from PanelAppRex to obtain the disease-related inheritance mode for each gene. For each gene, if no variant was observed for a given ClinVar classification (i.e. $p_i = 0$), a minimal risk was assigned as described above. Finally, we computed the occurrence probability, expected cases, and the probability of observing at least one case using the equations presented.

The final results were aggregated by gene and ClinVar classification and used to generate summary statistics that reviewed the predicted disease observation probabilities.

2.2 Validation of Autosomal Dominant Estimates Using *NFKB1*

To validate our genome-wide probability estimates in an autosomal dominant gene, we focused on *NFKB1*. Our goal was to compare the expected number of *NFKB1*-related CVID cases, as predicted by our framework, with the reported case count in a well-characterised national-scale PID cohort.

1. Reference Dataset. We used a reference dataset reported by Tuijnenburg et al. (19) to build a validation model in an autosomal dominant disease gene. A whole-genome sequencing study of 846 predominantly sporadic, unrelated primary immunodeficiency disease (PID) cases from the NIHR BioResource–Rare Diseases cohort identified *NFKB1* as one of the genes most strongly associated with PID. Sixteen novel heterozygous variants-including truncating, missense, and gene deletion variants-in *NFKB1* were found, accounting for 46% of common variable immunodeficiency (CVID) cases (n = 390) in the cohort.

Functional analyses, including structural protein evaluation, immunophenotyping, immunoblotting, and ex vivo lymphocyte stimulation, revealed that all carriers exhibited deficiencies in B-lymphocyte differentiation, particularly an increased CD21low B-cell population. These findings had established heterozygous loss-of-function variants in *NFKB1* as the most common monogenic cause of CVID, with significant prognostic implications.

2. Cohort Prevalence Calculation. Therefore, we used this UK-based cohort of 846 unrelated PID patients where 390 cases of CVID were attributed to *NFKB1*, yielding an observed cohort prevalence of

$$\text{Prevalence}_{\text{cohort}} = \frac{390}{846} \approx 0.461.$$

3. National Estimate Based on Literature. Based on literature, the prevalence of CVID in the general population was estimated at approximately 1/25 000. For a UK population of $N_{\text{UK}} \approx 69\,433\,632$, the expected number of CVID cases was calculated as

$$E_{\text{CVID}} \approx \frac{69\,433\,632}{25\,000} \approx 2777.$$

Thus, the maximum expected number of *NFKB1*-related CVID cases in the entire population was estimated as

$$\text{Estimated } NFKB1 \text{ cases} \approx 2777 \times 0.461 \approx 1280,$$

with an approximate 95% confidence interval (derived from Wilson’s method) of 1188 to 1374 cases.

4. Bayesian Adjustment. Given that the clinical cohort was derived from a specialized setting-likely capturing nearly all PID cases-the observed 390 cases may have better represented the true burden. To reconcile these perspectives, we performed a Bayesian adjustment by combining the known cohort data with the national estimate. Specifically, we computed a weighted average to symbolically acknowledge potential uncertainty:

$$\text{Adjusted Estimate} = w \cdot 390 + (1 - w) \cdot 1280,$$

with w set to 0.9 to reflect a strong preference for the observed data. Additionally, we modelled the uncertainty in the observed prevalence using a beta distribution:

$$p \sim \text{Beta}(390 + 1, 846 - 390 + 1),$$

and generated 10 000 posterior samples to obtain a density distribution for the adjusted estimate.

5. Validation test. Thus, the expected number of *NFKB1*-related CVID cases derived from our genome-wide probability estimates was compared with the observed counts from the UK-based PID cohort. This comparison validated our framework for estimating disease incidence in autosomal dominant disorders.

2.3 Validation Study for Autosomal Recessive CF Using CFTR

To validate our framework for autosomal recessive diseases, we focused on cystic fibrosis (CF). For comparability sizes between the validation studies, we analysed the most common single nucleotide variant (SNV) in the *CFTR* gene, typically reported as “p.Arg117His” (GRCh38 Chr 7:117530975 G/A, MANE Select HGVS p.ENST00000003084.11: p.Arg117His). Our goal was to validate our genome-wide probability estimates by comparing the expected number of CF cases attributable to the p.Arg117His variant in CFTR with the nationally reported case count in a well-characterised disease cohort.

1. Expected Genotype Counts. Let p denote the allele frequency of the p.Arg117His variant and q denote the combined frequency of all other pathogenic CFTR variants, such that

$$q = P_{\text{tot}} - p \quad \text{with} \quad P_{\text{tot}} = \sum_{i \in \text{CFTR}} p_i.$$

Under Hardy–Weinberg equilibrium for an autosomal recessive trait, the expected frequencies were:

$$f_{\text{hom}} = p^2 \quad (\text{homozygous for p.Arg117His})$$

and

$f_{\text{comphet}} = 2pq$ (compound heterozygotes carrying p.Arg117His and another pathogenic allele).

For a population of size N (here, $N \approx 69\,433\,632$), the expected number of cases were:

$$E_{\text{hom}} = N \cdot p^2, \quad E_{\text{comphet}} = N \cdot 2pq, \quad E_{\text{total}} = E_{\text{hom}} + E_{\text{comphet}}.$$

2. Mortality Adjustment. Since CF patients experience increased mortality, we adjusted the expected genotype counts using an exponential survival model. With an annual mortality rate $\lambda \approx 0.004$ and a median age of 22 years, the survival factor was computed as:

$$S = \exp(-\lambda \cdot 22).$$

Thus, the mortality-adjusted expected genotype count became:

$$E_{\text{adj}} = E_{\text{total}} \times S.$$

3. Bayesian Uncertainty Simulation. To incorporate uncertainty in the allele frequency p , we modelled p as a beta-distributed random variable:

$$p \sim \text{Beta}(p \cdot \text{AN}_{\text{eff}} + 1, \text{AN}_{\text{eff}} - p \cdot \text{AN}_{\text{eff}} + 1),$$

using a large effective allele count (AN_{eff}) for illustration. By generating 10,000 posterior samples of p , we obtained a distribution of the literature-based adjusted expected counts, E_{adj} .

4. Bayesian Mixture Adjustment. Since the national registry may not capture all nuances (e.g., reduced penetrance) of CFTR-related disease, we further combined the literature-based estimate with the observed national count (714 cases from the UK Cystic Fibrosis Registry 2023 Annual Data Report) using a 50:50 weighting:

$$E_{\text{Bayes}} = 0.5 \times (\text{Observed Count}) + 0.5 \times E_{\text{adj}}.$$

5. Validation test. Thus, the expected number of *CFTR*-related CF cases derived from our genome-wide probability estimates was compared with the observed counts from the UK-based CF registry. This comparison validated our framework for estimating disease incidence in autosomal dominant disorders.

3 Results

3.1 Observation Probability Across Disease Genes

Our study demonstrated that by integrating large-scale annotation databases-such as gnomAD, ClinVar, and dbNSFP-with disease gene panels from PanelAppRex, we could systematically scan every disease-gene panel according to inheritance mode. By combining reference population allele frequencies with reported ClinVar clinical significance classifications, we calculated an expected “observation probability” for each single nucleotide variant (SNV). This probability represented the likelihood of encountering a variant of a given pathogenicity class for a specific phenotype.

In practice, our approach computed a simple observation probability for every SNV across the genome and was applicable to any disease-gene panel. Here, we focused on panels related to Primary Immunodeficiency or Monogenic Inflammatory Bowel Disease, using PanelAppRex panel ID 398 as a case study. We report the probability of disease observation for a total of 54,814 ClinVar variant classifications in 557 genes.

The results summarized in **Table 1** illustrated that our method yielded a robust estimation of the probability of observing a variant with a particular ClinVar classification. This integrated framework enabled comprehensive analyses across the entire genome, paving the way for rapid assessment of variant significance in diverse disease contexts.

Table 1: Example of the first several rows from our main results for 557 genes of PanelAppRex’s panel: (ID 398) Primary immunodeficiency or monogenic inflammatory bowel disease. “ClinVar Significance” indicates the pathogenicity classification assigned by ClinVar, while “inVar Significance” indicates the pathogenicity classification assigned by ClinVar, while “Occurrence Prob” represents our calculated probability of observing the corresponding variant class for a given phenotype. Additional column including population allele frequency are not shown.

Gene	Panel ID	ClinVar Clinical Significance	GRCh38 Pos	HGVSc (VEP)	HGVSp (VEP)	Inheritance	Occurrence Probability
ABI3	398	Uncertain significance	49210771	c.47G>A	p.Arg16Gln	AR	0.000000007
ABI3	398	Uncertain significance	49216678	c.265C>T	p.Arg89Cys	AR	0.000000005
ABI3	398	Uncertain significance	49217742	c.289G>A	p.Val97Met	AR	0.000000002
ABI3	398	Uncertain significance	49217781	c.328G>A	p.Gly110Ser	AR	0.000000002
ABI3	398	Uncertain significance	49217844	c.391C>T	p.Pro131Ser	AR	0.000000015
ABI3	398	Uncertain significance	49220257	c.733C>G	p.Pro245Ala	AR	0.000000022

3.2 Validation of Dominant Disease Occurrence with *NFKB1*

To validate our genome-wide probability estimates for autosomal dominant disorders, we focused on *NFKB1*. We used a reference dataset from Tuijnenburg et al. (19), in which whole-genome sequencing of 846 PID patients identified *NFKB1* as one of the

genes most strongly associated with the disease, with 390 CVID cases attributed to heterozygous variants. Our goal was to compare the predicted number of *NFKB1*-related CVID cases with the reported count in this well-characterised national-scale cohort.

Our model calculated 456 *NFKB1*-related CVID cases in the UK. In the reference cohort, 390 *NFKB1* CVID cases were reported. We additionally wanted to account for potential under-reporting in the reference study. We used an extrapolated national CVID prevalence to yield an upper bound maximum of 1280 cases (95% CI: 1188–1374), while a Bayesian-adjusted mixture estimate produced a median of 835 cases (95% CI: 789–882). **Figure 1 (A)** illustrates that our predicted value of 456 lies within these ranges and is closer to the observed count, thereby supporting the validity of our integrated probability estimation framework for autosomal dominant disorders.

3.3 Validation of Recessive Disease Occurrence with *CFTR*

Our analysis predicted the number of cystic fibrosis (CF) cases attributable to carriage of the p.Arg117His variant (either as homozygous or as compound heterozygous with another pathogenic allele) in the UK. Based on Hardy–Weinberg calculations and mortality adjustments, we predicted approximately 648 cases arising from biallelic variants and 160 cases from homozygous variants, resulting in a total of 808 expected cases.

In contrast, the nationally reported number of CF cases was 714, as recorded in the UK Cystic Fibrosis Registry 2023 Annual Data Report. To account for factors such as reduced penetrance and the mortality-adjusted expected genotype, we derived a Bayesian-adjusted estimate via posterior simulation. Our Bayesian approach yielded a median estimate of 740 cases (95% CI: 696, 786) and a mixture-based estimate of 727 cases (95% CI: 705, 750).

Figure 1 (B) illustrates the close concordance between the predicted values, the Bayesian-adjusted estimates, and the national report supports the validity of our integrated approach for estimating disease incidence from population allele frequency data.

The density-scatter plot (**Figure 2**) shows the final values for these genes of interest in a given population size and phenotype. It reveals that an allele frequency threshold of approximately 0.000007 is required to observe a single heterozygous disease-causing variant carrier in the UK population for both genes. However, owing to the autosomal recessive inheritance pattern of *CFTR*, this threshold translates into more than 100,000 heterozygous carriers, compared to only 456 carriers for the autosomal dominant gene *NFKB1*. Note that this allele frequency threshold - being derived from the current reference population - represents a lower bound that can become more precise as public datasets continue to grow. This marked difference underscores the significant impact of inheritance patterns on population carrier frequencies and the observed disease prevalence.

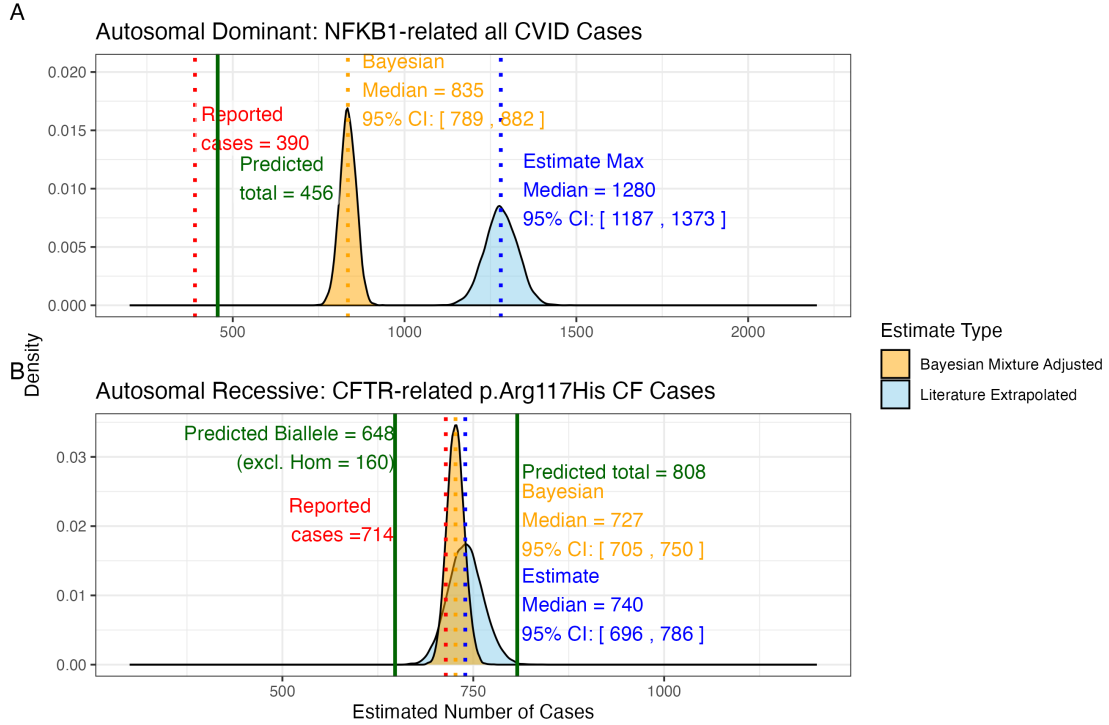


Figure 1: (A) Density distributions for the number of *NFKB1*-related CVID cases in the UK. Our model (green) predicted 456 cases, which falls between the observed cohort count (red) of 390 and the upper extrapolated values. The blue curve represents maximum count of 1280, and the orange curve shows the Bayesian-adjusted mixture estimate of 835. (B) Density distributions for *CFTR*-related p.Arg117His CF cases. Our model (green) predicted 648 biallelic cases and 808 total cases. The nationally reported case count (red) was 714. The blue curve represents maximum extrapolated count of 740, and the orange curve shows the Bayesian-adjusted mixture estimate of 727. We observed close agreement among the reported disease cases and our integrated probability estimation framework.

3.4 Interpretation of ClinVar Variant Observations

Figure 3 shows the two validation study PID genes, representing autosomal recessive and dominant inheritance. **Figure 3 (A)** illustrates the overall probability of an affected birth by ClinVar variant classification, whereas **Figure 3 (B)** depicts the total expected number of cases per classification for an example population, here the UK, of approximately 69.4 million. While true positive pathogenic variants are typically straightforward to confirm, benign variants or variants of uncertain significance (VUS) may be overemphasized if their interpretation relies solely on the prominence of the associated gene. A variant may seem clinically significant simply because it occurs in a well-known gene, even if its empirical occurrence probability is high, suggesting benignity. This view underscores the necessity of considering the prior probability of variant occurrence when assessing pathogenicity.

Condition: population size 69433632, phenotype PID-related, genes CFTR and NFKB1.

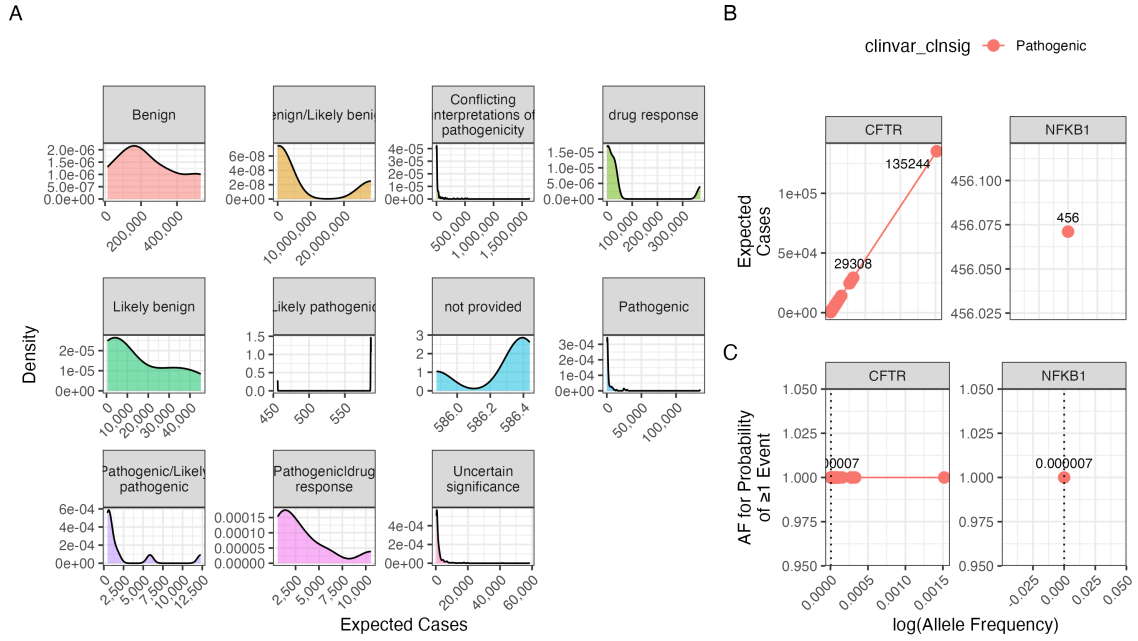


Figure 2: Interpretation of probability of observing a variant classification. The result from the chosen validation genes *CFTR* and *NFKB1* are shown. Case counts are dependant on the population size and phenotype. (A) The density plots of expected observations by ClinVar clinical significance. We then highlight the values for pathogenic variants specifically showing; (B) the allele frequency versus expected cases in this population size and (C) the probability of observing at least one event in this population size.

Recessive and Dominant Disease Genes

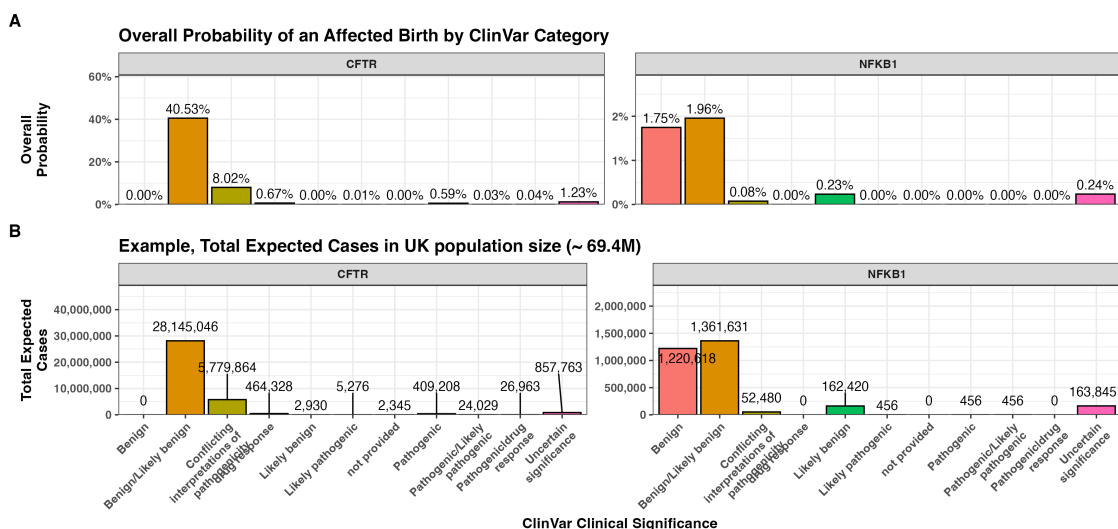


Figure 3: Combined bar charts summarizing the genome-wide analysis of ClinVar clinical significance for the PID gene panel. Panel (A) shows the overall probability of an affected birth by variant classification, and Panel (B) displays the total expected number of cases per classification, both stratified by gene. These integrated results illustrate the variability in variant observations across genes and underpin our validation of the probability estimation framework.

4 Discussion

In this study we focused on reporting the probability of disease observation for the disease gene panel (ID 398) primary immunodeficiency or monogenic inflammatory bowel disease. We report a total of 54814 ClinVar variant classifications in 557 genes. This thorough example of a query disease phenotype demonstrates how we can additionally run through all gene-disease combinations genome wide.

Our study employs classical genetic estimation using HWE to yield accurate, genome-wide probabilities of disease occurrence for SNVs. These estimates form robust priors for Bayesian models. The integration of variant interpretation guidelines, such as those provided by the ACMG (3) and complementary frameworks (4; 20), can be applied to generate clinically relevant outcomes.

Standardised variant interpretation protocols that incorporate quality control and filtering criteria (5; 6) are essential for robust genomic analysis. The concept of qualifying variants (QVs) (4; 7) plays a central role in filtering and interpreting SNVs, while statistical approaches such as ACAT and SKAT (9–12) offer robust tools for aggregating variant effects in association studies. Moreover, multi-block data fusion techniques enable the integration of DNA, RNA, and proteomic data for comprehensive variant interpretation (13; 14). Standardised reporting for QV sets (e.g., using ACMG Secondary Finding v3.2) (15) can be supplemented with the observation probabilities.

We acknowledge that our current approach focuses solely on SNVs and does not incorporate complex variants or an accurate estimate for de novo events. Future studies will address these limitations by incorporating additional models and data sources. By integrating these classical-style estimates with prior knowledge we can update probabilities continuously, ultimately enhancing the precision of genetic diagnostics.

References

- [1] Oliver Mayo. A Century of Hardy–Weinberg Equilibrium. *Twin Research and Human Genetics*, 11(3):249–256, June 2008. ISSN 1832-4274, 1839-2628. doi: 10.1375/twin.11.3.249. URL https://www.cambridge.org/core/product/identifier/S1832427400009051/type/journal_article.
- [2] Nikita Abramovs, Andrew Brass, and May Tassabehji. Hardy-Weinberg Equilibrium in the Large Scale Genomic Sequencing Era. *Frontiers in Genetics*, 11:210, March 2020. ISSN 1664-8021. doi: 10.3389/fgene.2020.00210. URL <https://www.frontiersin.org/article/10.3389/fgene.2020.00210/full>.
- [3] Sue Richards, Nazneen Aziz, Sherri Bale, David Bick, Soma Das, Julie Gastier-Foster, Wayne W Grody, Madhuri Hegde, Elaine Lyon, Elaine Spector, et al. Standards and guidelines for the interpretation of sequence variants: a joint consensus recommendation of the american college of medical genetics and genomics and the association for molecular pathology. *Genetics in medicine*, 17(5):405–423, 2015.
- [4] Sean V Tavtigian, Steven M Harrison, Kenneth M Boucher, and Leslie G Biesecker. Fitting a naturally scaled point system to the acmg/amp variant classification guidelines. *Human mutation*, 41(10):1734–1737, 2020.
- [5] Brent S Pedersen, Joe M Brown, Harriet Dashnow, Amelia D Wallace, Matt Velinder, Martin Tristani-Firouzi, Joshua D Schiffman, Tatiana Tvrdik, Rong Mao, D Hunter Best, et al. Effective variant filtering and expected candidate variant yield in studies of rare human disease. *NPJ Genomic Medicine*, 6(1):1–8, 2021.
- [6] Carl A Anderson, Fredrik H Pettersson, Geraldine M Clarke, Lon R Cardon, Andrew P Morris, and Krina T Zondervan. Data quality control in genetic case-control association studies. *Nature protocols*, 5(9):1564–1573, 2010. URL <https://doi.org/10.1038/nprot.2010.116>.
- [7] Elizabeth T Cirulli, Brittany N Lasseigne, Slavé Petrovski, Peter C Sapp, Patrick A Dion, Claire S Leblond, Julien Couthouis, Yi-Fan Lu, Quanli Wang, Brian J Krueger, et al. Exome sequencing in amyotrophic lateral sclerosis identifies risk genes and pathways. *Science*, 347(6229):1436–1441, 2015.
- [8] Gundula Povysil, Slavé Petrovski, Joseph Hostyk, Vimla Aggarwal, Andrew S. Allen, and David B. Goldstein. Rare-variant collapsing analyses for complex traits: guidelines and applications. *Nature Reviews Genetics*, 20(12):747–759, 2019. doi: 10.1038/s41576-019-0177-4. URL <https://doi.org/10.1038/s41576-019-0177-4>.
- [9] Yaowu Liu, Sixing Chen, Zilin Li, Alanna C Morrison, Eric Boerwinkle, and Xihong Lin. Acat: a fast and powerful p value combination method for rare-

variant analysis in sequencing studies. *The American Journal of Human Genetics*, 104(3):410–421, 2019.

- [10] Xihao Li, Zilin Li, Hufeng Zhou, Sheila M Gaynor, Yaowu Liu, Han Chen, Ryan Sun, Rounak Dey, Donna K Arnett, Stella Aslibekyan, et al. Dynamic incorporation of multiple in silico functional annotations empowers rare variant association analysis of large whole-genome sequencing studies at scale. *Nature genetics*, 52(9):969–983, 2020.
- [11] Michael C Wu, Seunggeun Lee, Tianxi Cai, Yun Li, Michael Boehnke, and Xihong Lin. Rare-variant association testing for sequencing data with the sequence kernel association test. *The American Journal of Human Genetics*, 89(1):82–93, 2011.
- [12] Seunggeun Lee, Mary J Emond, Michael J Bamshad, Kathleen C Barnes, Mark J Rieder, Deborah A Nickerson, David C Christiani, Mark M Wurfel, and Xihong Lin. Optimal unified approach for rare-variant association testing with application to small-sample case-control whole-exome sequencing studies. *The American Journal of Human Genetics*, 91(2):224–237, 2012.
- [13] Augustine Kong, Gudmar Thorleifsson, Michael L Frigge, Bjarni J Vilhjalmsson, Alexander I Young, Thorgeir E Thorgeirsson, Stefania Benonisdottir, Asmundur Oddsson, Bjarni V Halldorsson, Gisli Masson, et al. The nature of nurture: Effects of parental genotypes. *Science*, 359(6374):424–428, 2018.
- [14] Laurence J Howe, Michel G Nivard, Tim T Morris, Ailin F Hansen, Humaira Rasheed, Yoonsu Cho, Geetha Chittoor, Penelope A Lind, Teemu Palviainen, Matthijs D van der Zee, et al. Within-sibship gwas improve estimates of direct genetic effects. *BioRxiv*, pages 2021–03, 2021.
- [15] David T Miller, Kristy Lee, Noura S Abul-Husn, Laura M Amendola, Kyle Brothers, Wendy K Chung, Michael H Gollob, Adam S Gordon, Steven M Harrison, Ray E Hersherberger, et al. Acmg sf v3. 2 list for reporting of secondary findings in clinical exome and genome sequencing: a policy statement of the american college of medical genetics and genomics (acmg). *Genetics in Medicine*, 25(8):100866, 2023.
- [16] Dylan Lawless. PanelAppRex aggregates disease gene panels and facilitates sophisticated search. March 2025. doi: 10.1101/2025.03.20.25324319. URL <http://medrxiv.org/lookup/doi/10.1101/2025.03.20.25324319>.
- [17] Melissa J Landrum, Jennifer M Lee, Mark Benson, Garth R Brown, Chen Chao, Shanmuga Chitipiralla, Baoshan Gu, Jennifer Hart, Douglas Hoffman, Wonhee Jang, Karen Karapetyan, Kenneth Katz, Chunlei Liu, Zenith Maddipatla, Adriana Malheiro, Kurt McDaniel, Michael Ovetsky, George Riley, George Zhou, J Bradley Holmes, Brandi L Kattman, and Donna R Maglott. ClinVar: improving access to variant interpretations and supporting evidence. *Nucleic Acids*

Research, 46(D1):D1062–D1067, January 2018. ISSN 0305-1048, 1362-4962. doi: 10.1093/nar/gkx1153. URL <http://academic.oup.com/nar/article/46/D1/D1062/4641904>.

- [18] Xiaoming Liu, Chang Li, Chengcheng Mou, Yibo Dong, and Yicheng Tu. dbNSFP v4: a comprehensive database of transcript-specific functional predictions and annotations for human nonsynonymous and splice-site SNVs. *Genome Medicine*, 12(1):103, December 2020. ISSN 1756-994X. doi: 10.1186/s13073-020-00803-9. URL <https://genomemedicine.biomedcentral.com/articles/10.1186/s13073-020-00803-9>.
- [19] Paul Tuijnenburg, Hana Lango Allen, Siobhan O. Burns, Daniel Greene, Machiel H. Jansen, and Others. Loss-of-function nuclear factor B subunit 1 (NFKB1) variants are the most common monogenic cause of common variable immunodeficiency in Europeans. *Journal of Allergy and Clinical Immunology*, 142(4):1285–1296, October 2018. ISSN 00916749. doi: 10.1016/j.jaci.2018.01.039. URL <https://linkinghub.elsevier.com/retrieve/pii/S0091674918302860>.
- [20] Quan Li and Kai Wang. Intervar: clinical interpretation of genetic variants by the 2015 acmg-amp guidelines. *The American Journal of Human Genetics*, 100(2):267–280, 2017.